MARCEL DEKKER, INC. • 270 MADISON AVENUE • NEW YORK, NY 10016

©2002 Marcel Dekker, Inc. All rights reserved. This material may not be used or reproduced in any form without the express written permission of Marcel Dekker, Inc.

synthetase (eNOS) by VEGF, but did not inhibit p38 activation by the VEGFR-1-specific ligand, placental growth factor (PlGF). Inhibition of VEGFR-2 also perturbed VEGF-induced membrane extension, cell migration, and tube formation by HAECs. Vascular endothelial growth factor receptor-2 inhibition also reversed VEGF-stimulated phosphorylation of CrkII and its Src homology 2 (SH2)-binding protein $p130^{Cas}$, which are known to play a pivotal role in regulating endothelial cell migration. Inhibition of VEGFR-2 thus blocked all VEGF-induced endothelial cellular responses tested, supporting that the catalytic activity of VEGFR-2 is critical for VEGF signaling and/or that VEGFR-2 may function in a heterodimer with VEGFR-1 in human vascular endothelial cells.

Key Words: VEGF receptor; Inhibitor; Angiogenesis.

INTRODUCTION

The vascular endothelial growth factor receptor (VEGFR) family consists of VEGFR-1/Flt-1, VEGFR-2/Flk-1/KDR, and VEGFR-3/Flt-4 (1). Among them, VEGFR-1 and -2 expressed mainly in vascular endothelial cells are essential for vascular development, as shown by the disruption of each gene (2,3). Vascular endothelial growth factor receptor-3 is exclusively expressed in lymphatic endothelial cells (4). VEGFR-2 is thought to be responsible for VEGF-stimulation of vascular endothelial cells based on knockout of VEGFR-1 or -2 genes (5), overexpression of VEGFR-1 or -2 (6), and use of VEGFR-1 or -2-specific ligands (7); however, it remains unclear which receptor, VEGFR-1 or -2, is necessary and sufficient for angiogenic signals that control endothelial proliferation and migration.

Mitogen-activated protein kinases (MAPKs) regulate gene expression, cell proliferation or survival, and the cell cycle. The MAPK family consists of extracellular signal regulated-kinase (ERK), c-jun NH_2-terminal kinase (JNK), and p38 (stress-activated kinase 2) (8). Vascular endothelial growth factor-stimulated endothelial cells show the activation of ERK and p38 but not JNK (9). Extracellular regulated-kinase activation is critical for cell proliferation, whereas p38 is essential for the formation of stress fibers and focal adhesions (9). Recent data has shown that VEGF-induced ERK activation is independent of Ras activation but dependent on the phospholipase Cγ (PLCγ)-protein kinase C (PKC)-Raf pathway (10).

Akt activation is critical for VEGF-induced cell motility and cell survival (11,12). Akt functions downstream of phosphatidylinositol-3-kinase (PI3-K) and phosphorylates a wide variety of substrates on serine/threonine residues, including Bad that regulates apoptosis, p21-activated protein kinase (PAK) that controls the cell cycle, and endothelial nitric oxide synthetase (eNOS) that modulates vascular smooth muscle relaxation via guanylate cyclase (13). Recently, Akt has been shown to phosphorylate the endothelial cell differentiation gene (EDG) receptor that activates Rac via PI3-K (14). Rac induces membrane ruffling and subsequent cell migration (15). Furthermore, PAK, an effector of Rac, regulates actin cytoskelton reorganization. Thus, Akt functions as a regulator for VEGF-stimulated endothelial cell migration.

The adaptor protein CrkII consists of a Src homology 2 (SH2) domain and two SH3 domains (16). CrkI is an alternatively spliced variant of *crk gene* and consists of the same SH2 and amino-terminal SH3 domain as CrkII. The Crk SH3-binding protein DOCK180

©2002 Marcel Dekker, Inc. All rights reserved. This material may not be used or reproduced in any form without the express written permission of Marcel Dekker, Inc.

promotes guanine nucleotide exchange for Rac and accelerates membrane extension (17). CrkII SH2-binding proteins, $p130^{Cas}$, and paxillin are involved in regulation of cell motility. $p130^{Cas}$ together with CrkII accelerates the cell migration, whereas paxillin reduces the cell motility (18). VEGFR-1 contains tyrosine residues which potentially bind CrkII SH2 (19). Vascular endothelial growth factor receptor-2 is also suggested to associate either directly or indirectly with CrkII (20).

We have delineated signaling from VEGFR-2 by using a novel VEGFR-2-selective inhibitor, ZM323881, and demonstrated that VEGFR-2 is required for ERK activation, Akt phosphorylation, and CrkII phosphorylation in VEGF-stimulated human aortic endothelial cells (HAECs). We further show that VEGFR-2 is responsible for endothelial cell migration and subsequent tube formation of HAECs on matrigel.

MATERIALS AND METHODS

Reagents and Antibodies

The following were purchased from Calbiochem: AG1478, an inhibitor of epidermal growth factor receptor (EGFR) kinase; SU5614, an inhibitor of platelet-derived growth factor receptor (PDGFR) kinase and VEGFR kinase; VEGFR kinase inhibitor (VEGF-TKI), an inhibitor of both VEGFR-1 and -2 kinases. ZM323881 was provided by Dr. Anderson Ryan (AstraZeneca, UK). Recombinant human $VEGF_{165}$ (hereafter, VEGF) and recombinant human placental growth factor (PlGF) were purchased from R&D systems. Hepatocyte growth factor (HGF), epidermal growth factor (EGF), and platelet-derived growth factor-β (PDGF-β) were from Sigma. Anti-phospho-p44/42 mitogen activated protein kinase (ERK) antibody, anti-Phospho-EGFR (Tyr1068) antibody, anti-phospho-Akt (Ser473) antibody, anti-phospho-eNOS (Ser1177) antibody, anti-Akt antibody; and anti-p38 antibody were from Cell Signaling Technology; anti-Crk antibody, anti-eNOS antibody, anti-phosphotyrosine antibody (PY20), and anti-$p130^{Cas}$ antibody were from Transduction Laboratories; anti-ACTIVE-p38 antibody was from Promega; anti-ERK antibody, anti-HGFR antibody (anti-human Met extracellular region antibody), and anti-PDGFR were from Upstate Technology; anti-phospho VEGFR-2 antibody was from Oncogene Research Products; anti-VEGFR-1 antibody was from Santa Cruz Biotechnology; peroxidase-conjugated goat anti-mouse IgG and goat anti-rabbit IgG were from Amersham Bioscience.

Plasmids, Adenovirus, and Cell Culture

pCXN2-FLAG-CrkI-W169L-IRES-EGFP expressing CrkI consisting of an intact SH2 and a nonfunctional SH3 and enhanced green fluorescent protein (EGFP) was constructed previously (21). Adenovirus expressing GFP was a kind gift from H. Kurose (Kyushu University, Japan). Human aortic endothelial cells and NIH3T3 cells were purchased from Cascade Biologics and Japan Cell Resource Bank, respectively. HAECs were maintained in HuMedia-EG2 (Kurabo, Japan) as described previously. NIH3T3 cells were cultured in Dulbecco's Eagle's Medium (DMEM) containing 10% fetal bovine serum and 2 mmol/L

MARCEL DEKKER, INC. • 270 MADISON AVENUE • NEW YORK, NY 10016
©2002 Marcel Dekker, Inc. All rights reserved. This material may not be used or reproduced in any form without the express written permission of Marcel Dekker, Inc.

L-glutamine. HAECs were used before passage 7. HAECs were transfected with plasmids using Lipofect-AMINE plus (Invitrogen).

Immunoblotting and Immunoprecipitation

HAECs or NIH3T3 cells were stimulated by reagents with or without pretreatment as indicated in the figure legends. Immunoblotting and immunoprecipitation was performed as described previously (21). Briefly, cells were lysed in lysis buffer (1% Triton X-100, 150 mmol/L NaCl, 25 mmol/L *tris* hydrochloride (pH 7.5), 1.5 mmol/L $MgCl_2$, 1 mmol/L Na_3VO_4, 10 mmol/L NaF, and protease inhibitor cocktail (Roche Diagnostics), precleared by centrifugation for 10 min at 15,000 *g*. Lysates were subjected to SDS-PAGE and immunoblotted with antibodies indicated at the figures. Remaining lysates were immunoprecipitaed and immunoblotted with the antibodies as indicated. Immunoreactive bands were visualized by the ECL system (Amersham Biosciences). Bands were quantified using the LAS-1000 system (Fuji Film, Japan).

Time-lapse Imaging, Quantitative Analysis of Membrane Extension, and Cell Motility Analysis

The motility of HAECs was analyzed as described previously (21). HAECs infected with recombinant GFP expressing adenovirus were spread on a collagen-coated glass base dish and cultured in DMEM supplemented with 0.5% bovine serum albumin for 8 hours with or without pretreatment using ZM323881 and exposed to VEGF for 6 hours in the presence or absence of ZM323881. GFP-expressing HAECs were tracked using fluorescent microscopy (Olympus IX-71). Both phase contrast images and epifluorescent images were collected every 30 s as a series of time-lapse images using MetaMorph 4.6 software (Roper Scientific). These images were converted to a video using MetaMorph 4.6 software. The migratory speed of VEGF-stimulated HAECs was calculated using cell-tracking system included in the MetaMorph 4.6 software. Vascular endothelial growth factor-induced membrane extension reflecting membrane ruffling was quantified by measuring the size before and after the stimulation, as described previously (21). The cell size was analyzed by a region measurement tool included in the MetaMorph 4.6 software.

Tube Formation Assay on Matrigel

Tube formation was tested on the matrigel (Becton Dickinson) in the presence or absence of ZM323881 as described (22). Briefly, 150 μL of matrigel on a glass base dish was polymerized at 37°C for 30 min. 1×10^5 HAECs in 100 μL DMEM containing VEGF or HGF were added to the matrigel with or without ZM323881. The area covered by the tube was quantified by the use of MetaMorph 4.6 software.

Statistics

All experiments were repeated at least three times. The statistical significance was evaluated by Student's *t*-test.

MARCEL DEKKER, INC. • 270 MADISON AVENUE • NEW YORK, NY 10016

©2002 Marcel Dekker, Inc. All rights reserved. This material may not be used or reproduced in any form without the express written permission of Marcel Dekker, Inc.

RESULTS

VEGF-induced ERK and p38 Activation Depend on VEGFR-2 But Not on VEGFR-1

ZM323881 [Fig. 1(A)] is an anilinoquinazoline that potently inhibits VEGFR-2 tyrosine kinase activity and shows a high degree of selectivity over other receptor tyrosine kinases, including VEGFR-1 (IC(50) < 2 nM) (23,24). Here, we characterized the effect of ZM323881 on VEGF-induced signaling in HAECs.

HAECs were stimulated with 40 ng/mL of VEGF in the presence of ZM323881 or SU5614, an inhibitor of both VEGFR and PDGFR tyrosine kinases, at the concentration indicated at the top of the figure. ZM323881 completely inhibited VEGF-induced ERK phosphorylation at 1 μmol/L like SU5614 [Fig. 1(B)]. Thus, a dose of 1 μmol/L ZM323881 was used in all the following studies. Ineffectiveness to HGFR was indicated by the observation that HGF-induced ERK activation was not inhibited by ZM323881 [Fig. 1(C), center]. PlGF, which activated VEGFR-1 but not VEGFR-2, did not induce ERK phosphorylation in HAECs [Fig. 1(C), right]. Although VEGF, HGF, and PlGF induced p38 phosphorylation, only VEGF-induced p38 phosphorylation was inhibited by ZM323881, suggesting that ZM323881 inhibited VEGFR-2, but not HGFR and VEGFR-1 [Fig. 1(D)]. Furthermore, we examined whether ligand-stimulated VEGFR-1, VEGFR-2, and HGFR phosphorylation was inhibited by ZM323881. HAECs stimulated with VEGF in the absence or presence of ZM323881 were immunoprecipitated by anti-phosphotyrosine antibody and immunoprecipitates were immunoblotted with anti-phospho-VEGFR-2 antibody [Fig. 1(E), left]. VEGF-induced VEGFR-2 phosphorylation was abolished by ZM323881. When HAECs were stimulated with HGF [Fig. 1(E), center] in a similar manner to VEGF [Fig. 1(E), center], HGFR phosphorylation was not inhibited by ZM323881. In addition, we tested the effect of ZM323881 on PlGF-induced phosphorylation of VEGFR-1. M323881 did not inhibit VEGFR-1 phosphorylation by PlGF, while VEGF-TKI, a kinase inhibitor for both VEGFR-1 and -2, inhibited. These results demonstrate that ZM323881 inhibits VEGFR-2-dependent ERK and p38 activation but not VEGFR-1-dependent p38 activation or HGF-induced ERK and p38 activation in HAECs.

Neither PDGFR Nor EGFR Is Inhibited by ZM323881

We examined the selectivity of ZM323881 over other receptor tyrosine-kinases, PDGFR and EGFR in NIH3T3 cells. PDGF-induced ERK activation was not inhibited by ZM323881 while SU5614, an inhibitor for PDGFR and VEGFR, inhibited PDGF-induced ERK activation [Fig. 2(A)]. Similarly, EGF-induced ERK activation was inhibited by AG1478, an inhibitor for EGFR tyrosine kinase, but not by ZM323881 [Fig. 2(B)]. Neither PDGF- nor EGF-induced ERK activation was inhibited by ZM323881 even at 50 times higher concentration (50 μmol/L) than the concentration effective for VEGFR-2 tyrosine kinase. NIH3T3 cells were stimulated with PDGF-β in the presence of either ZM323881 or SU5614. PDGFR-β phosphorylation was inhibited by SU5614 but not ZM323881 [Fig. 2(C), left]. Similarly, NIH3T3 cells were stimulated with EGF in the presence of either ZM323881 or AG1478. EGFR phosphorylation was inhibited by AG1478, but not

©2002 Marcel Dekker, Inc. All rights reserved. This material may not be used or reproduced in any form without the express written permission of Marcel Dekker, Inc.

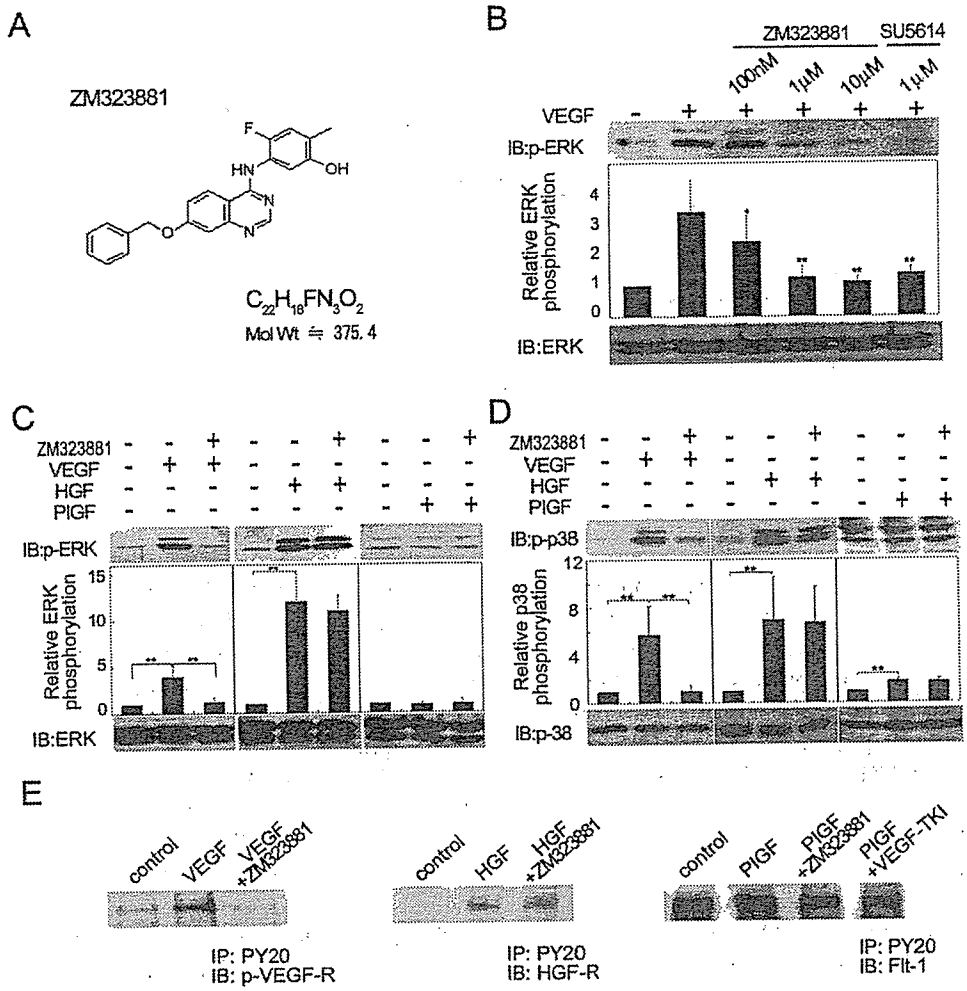

Figure 1. Specific inhibitory effect of ZM323881 on VEGFR-2-mediated ERK and p38 activation. (A) Chemical structure of ZM323881. (B) HAECs were pretreated with ZM323881 or SU5614, an inhibitor for both VEGFR and PDGFR, for 30 min prior to exposure to 40 mg/mL VEGF for 3 min. VEGF-induced ERK activation was examined by immunoblotting (IB) with anti-phospho-ERK (p-ERK) antibody and was inhibited by ZM323881 as well as SU5614. (C) HAECs were stimulated with growth factors indicated at the top in the presence or absence of ZM323881. VEGF-induced ERK activation, but not HGF-induced ERK activation, was inhibited by ZM323881. (D) HAECs were stimulated as a similar manner to (C) and examined for the effect of ZM323881 on p38 activation. VEGF-induced p38 activation, but not either HGF- or PlGF-induced p38 activation, was inhibited by ZM323881. (E) HAECs were stimulated with growth factors as indicated at the top and immunoprecipitaed with anti-phosphotyrosine antibody (PY20). Immunoprecipitates were subjected to SDS-PAGE followed by immunoblotting with antibodies as indicated at the bottom. VEGF-induced VEGFR-2 phosphorylation was attenuated by ZM323881 (left), but neither HGF-induced HGFR phosphorylation (center) nor PlGF-induced VEGFR-1 phosphorylation (right) was inhibited by ZM323881. PlGF-induced VEGFR-1 phosphorylation was inhibited by VEGF-TKI. $*P < 0.05$, $**P < 0.01$. Immunoblot result is a representative of those performed at least three times.

©2002 Marcel Dekker, Inc. All rights reserved. This material may not be used or reproduced in any form without the express written permission of Marcel Dekker, Inc.

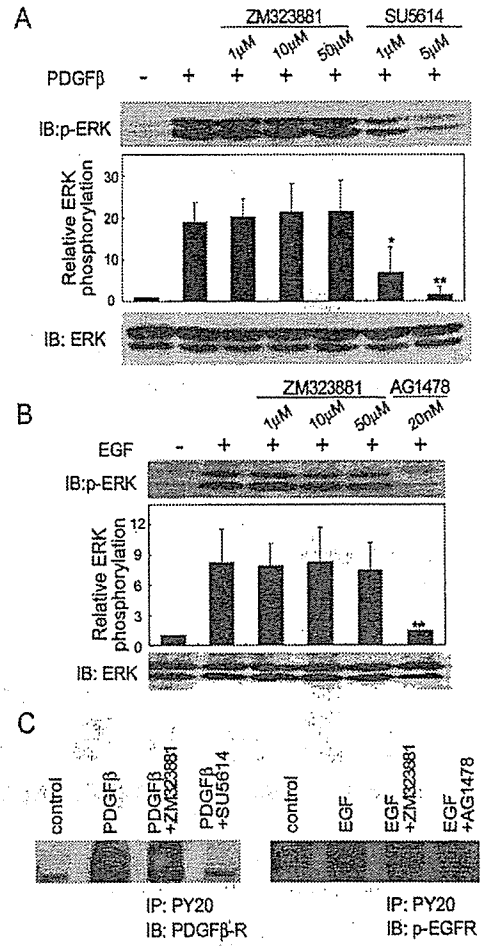

Figure 2. ZM323881 inhibits VEGFR-2 receptor tyrosine kinase but not PDGFR or EGFR tyrosine kinase. (A) NIH3T3 cells were pretreated with either 1 μmol/L ZM323881 or 1 μmol/L SU5614 prior to exposure to 20 mg/mL PDGFβ for 3 min. PDGF-β-induced ERK phosphorylation was inhibited by SU5614 but not by ZM323881. (B) EGF-induced ERK phosphorylation was inhibited by pretreatment with the EGFR-specific inhibitor AG1433, but not by ZM323881 in NIH3T3 cells. (C), Neither PDGFβ-induced PDGFR phosphorylation (left) nor EGF-induced EGFR phosphorylation (right) was inhibited by ZM323881. $^*P < 0.05$, $^{**}P < 0.01$.

ZM323881. These results indicated that ZM323881 did not significantly inhibit either PDGFR or EGFR tyrosine kinases.

VEGFR-2 Is Responsible for VEGF-Induced Akt and eNOS Activation

Akt activation contributes to angiogenesis (13). We examined whether VEGF-induced Akt phosphorylation and subsequent eNOS phosphorylation depend on VEGFR-1 or -2

©2002 Marcel Dekker, Inc. All rights reserved. This material may not be used or reproduced in any form without the express written permission of Marcel Dekker, Inc.

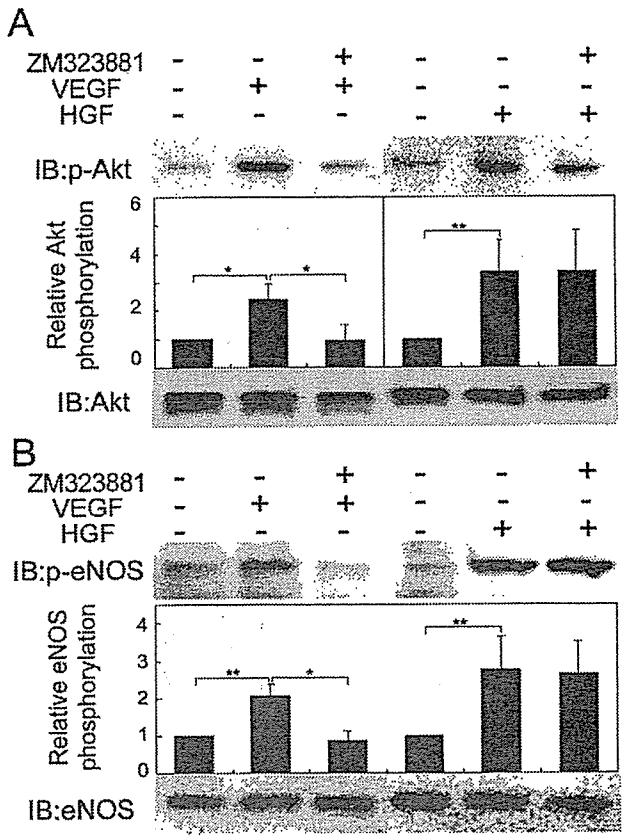

Figure 3. The inhibitory effect of ZM323881 on VEGF-induced Akt and eNOS phosphorylation. (A) HAECs were stimulated with either VEGF or HGF in the presence or absence of ZM323881. VEGF-induced Akt phosphorylation was examined using anti-phospho-Akt antibody (p-Akt) (top). Either VEGF- or HGF-induced phosphorylation of Akt over control was quantified (bottom). VEGF-induced Akt phosphorylation, but not HGF-induced Akt phosphorylation, was inhibited by ZM323881. $*P < 0.05$, $**P < 0.01$. (B) VEGF-induced eNOS phosphorylation was examined as a similar manner to (A). VEGF-induced eNOS phosphorylation, but not HGF-induced eNOS phosphorylation, was inhibited by ZM323881.

using ZM323881. Vascular endothelial growth factor-induced Akt phosphorylation and eNOS phosphorylation were completely abrogated by ZM323881, although those induced by HGF were not inhibited [Fig. 3(A) and (B)], indicating that VEGFR-2 was responsible for Akt phosphorylation and eNOS phosphorylation in HAECs stimulated with VEGF.

VGFR-2 Is Required for VEGF-Induced CrkII and $p130^{Cas}$ Phosphorylation

CrkII functions as an adaptor protein that links phosphotyrosine-containing molecules, including receptor tyrosine-kinases, $p130^{Cas}$, and paxillin, via its SH2 domain to

©2002 Marcel Dekker, Inc. All rights reserved. This material may not be used or reproduced in any form without the express written permission of Marcel Dekker, Inc.

effector molecules such as guanine nucleotide exchangers, C3G for Rap1 and DOCK180 for Rac, via amino-terminal SH3 domain. We tested whether CrkII is involved in VEGF-induced membrane extension, reflecting membrane ruffling proceeding cell migration. We have previously shown that dominant negative CrkI functions as both dominant negative CrkI and CrkII (21), because both CrkI and CrkII have the common SH2 and amino-terminal SH3 of CrkII. Untransfected HAECs responded to VEGF and showed membrane extension, whereas HAEC transfected with a dominant negative mutant of CrkI (green) did not exhibit membrane extension. We quantified the increase in cell size of untransfected HAECs and those transfected with pCXN2-FLAG-CrkI-IRES-EGFP in response to VEGF [Fig. 4(A), right]. These data indicated that CrkII was required for VEGF-induced membrane extension. We further tested whether VEGFR-2 was responsible for VEGF-induced CrkII phosphorylation. ZM323881 inhibited VEGF-induced CrkII phosphoryla-

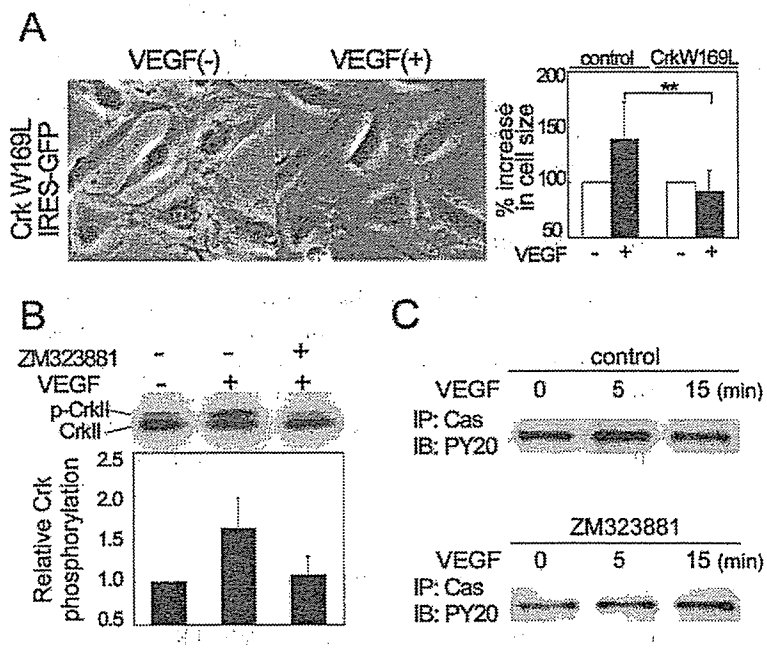

Figure 4. The requirement of CrkII and $p130^{Cas}$ for VEGF-induced membrane extension of HAECs. (A) HAECs expressing dominant negative CrkI (W169L) and EGFP did not show membrane extension in response to VEGF (left). VEGF-induced membrane extension was quantitatively analyzed in cells transfected with dominant negative CrkI (W169L) or control vector in the absence (−) or presence (+) of VEGF (right). (B) VEGF-induced CrkII phosphorylation was inhibited by ZM323881. Phosphorylated CrkII (p-CrkII) and non-phosphorylated CrkII (CrkII) were detected as slower- and faster-migrating forms of CrkII on the membrane probed with anti-Crk antibody (top). Relative Crk phosphorylation indicates the ratio of the post-stimulation phosphorylated fraction of total CrkII (CrkII and phosphorylated CrkII) to the pre-stimulation (control) phosphorylated-CrkII fraction. (C) HAECs stimulated with VEGF in the absence (top) or presence (bottom) of ZM323881 for the time indicated at the top were lysed and immunoprecipitated (IP) by anti-$p130^{Cas}$ antibody (Cas) and precipitates were immunoblotted with anti-phosphotyrosine (PY20). VEGF-induced $p130^{Cas}$ phosphorylation was inhibited by ZM323881. $^{**}P < 0.01$.

©2002 Marcel Dekker, Inc. All rights reserved. This material may not be used or reproduced in any form without the express written permission of Marcel Dekker, Inc.

tion [Fig. 4(B), top], as demonstrated by quantitation of relative CrkII phosphorylation indicating the ratio of the post-stimulation phosphorylated CrkII fraction of total CrkII (CrkII + phosphorylated CrkII) to the pre-stimulation (control) phosphorylated CrkII fraction [Fig. 4(B), bottom]. Next we examined the effect of ZM323881 on VEGF-induced $p130^{Cas}$ phosphorylation. VEGF induced $p130^{Cas}$ phosphorylation [Fig. 4(C), top]. ZM323881 inhibited VEGF-induced phosphorylation of $p130^{Cas}$ [Fig. 4(C), bottom].

VEGFR-2 Is Responsible for VEGF-Induced Membrane Extension and Cell Motility

Both CrkII and $p130^{Cas}$ are involved in cell migration. ZM323881 inhibited both CrkII and $p130^{Cas}$ phosphorylation. We therefore tested the effect of ZM323881 on VEGF-induced membrane extension and cell motility in HAECs. VEGF induced remarkable membrane extension in the absence of ZM323881 but not in the presence of ZM323881 [Fig. 5(A)]. We proceeded to measure the speed of cell movement induced by VEGF [Fig. 5(B)]. About 60% of unstimulated cells moves slower than 0.6 μm/min [Fig. 5(B), left], whereas about 60% of cells stimulated with VEGF moves faster than 0.6 μm/min [Fig. 5(B), center], indicating that VEGF accelerated cell migration. However, ZM323881 inhibited this VEGF-induced increase in cell motility [Fig. 5(B), right]. Therefore, VEGFR-2 is necessary for VEGF-induced endothelial cell migration.

VEGFR-2 Is Required for Tube-Formation on Matrigel

Endothelial cells on matrigel form capillary-like networks as shown in Fig. 6. Matrigel containing 40 ng/mL VEGF or 30 ng/mL HGF induced wide and long tube formations (Fig. 6, top center and top right). ZM323881 inhibited VEGF-induced tube formation but not that induced by HGF (Fig. 6, middle center and middle right). We quantified tube formation by measuring the area covered by tube-like structures on matrigel. ZM323881 significantly reduced the VEGF-induced tube formation, whereas it did not affect that induced by HGF (Fig. 6, bottom).

DISCUSSION

It has been difficult to determine which receptor, VEGFR-1, -2, or -3 mediates angiogenesis because VEGF family receptors redundantly respond to VEGF and its related factors including PlGF, VEGF-B, VEGF-C, VEGF-D, and VEGF-E (25,26). We demonstrate here, using ZM323881, that VEGF-activated intracellular signals that lead to cell proliferation and migration, which are important for angiogenesis, are dependent on VEGFR-2. Vascular endothelial growth factor receptor-2-specific inhibitor, ZM323881, has enabled us to delineate VEGFR-2 specific signals in endothelial cells stimulated with VEGF.

Angiogenesis requires endothelial cell migration. Cell migration is a sequential reorganization of cellular structures including membrane extension, assembly of cell contacts to extracellular matrices in the leading edge, and is accelerated by the increased locomotive force driven by acto-myosin coupling (27). Rac, one of the Rho family GTPases, is a key regulator for membrane extension. Rac is activated by both Dbl homology- and pleckstrin homology-containing molecules downstream of PI3-K (28) and/or by the CrkII-

©2002 Marcel Dekker, Inc. All rights reserved. This material may not be used or reproduced in any form without the express written permission of Marcel Dekker, Inc.

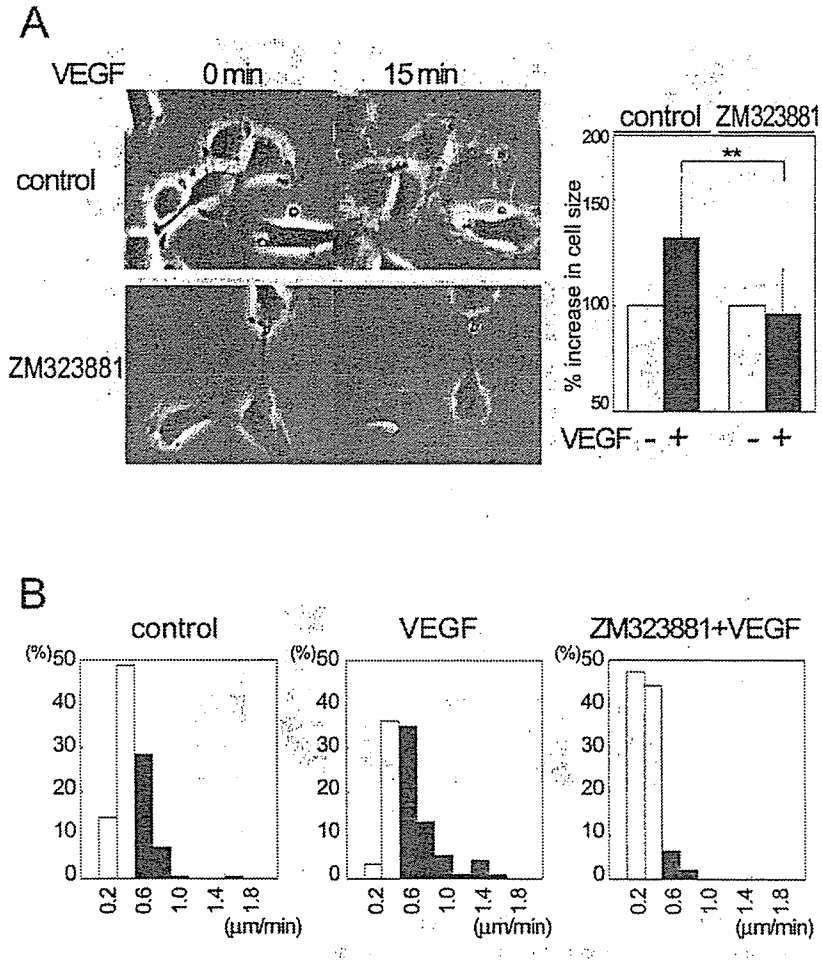

Figure 5. The requirement of VEGFR-2 for VEGF-induced membrane extension. (A) HAECs were imaged before (left) and after 15 min (right) to VEGF in the absence (top) or presence (bottom) of ZM323881. Arrowheads indicate the extended membrane. Quantitation of membrane extension induced by VEGF was shown in right panel, demonstrating that ZM323881 perturbed VEGF-induced membrane extension. (B) VEGF-induced acceleration of cell migration was inhibited by ZM323881. HAECs expressing EGFP was tracked and analyzed for their migration speed as described in Materials and Methods. HAECs moving faster than 0.6 μm/min. were indicated as black column. $^{**}P < 0.01$.

DOCK180 pathway (17). Akt is also activated downstream of PI3-K (29), although it is still controversial whether Akt functions upstream or downstream of Rac for cell migration (13).

VEGF activates PI3-K-mediated signaling in endothelial cells (30). We demonstrate that VEGF-induced Akt phosphorylation is dependent on VEGFR-2 (Fig. 3), as evidenced by that Akt phosphorylation by VEGF stimulation was abolished by pretreatment with ZM323881. Our data is consistent with previous studies showing that VEGFR-1-specific ligand, PlGF, does not induce Akt phosphorylation in endothelial cells (31). VEGFR-2 was

©2002 Marcel Dekker, Inc. All rights reserved. This material may not be used or reproduced in any form without the express written permission of Marcel Dekker, Inc.

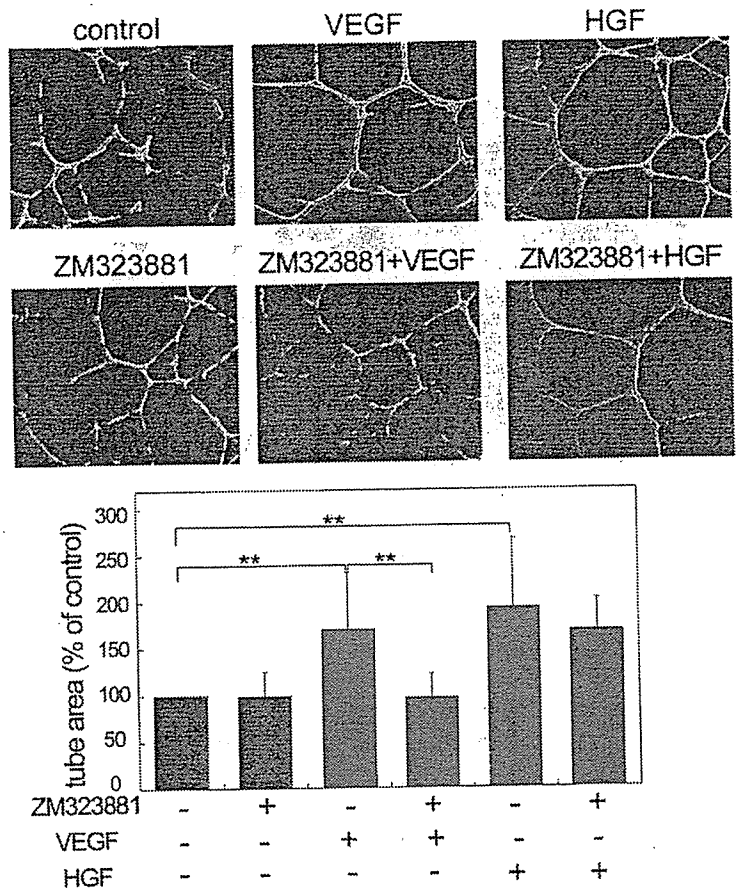

Figure 6. The inhibitory effect of ZM323881 on VEGF-induced tube formation on matrigel. VEGF- or HGF-induced tube formation on matrigel was imaged in the presence (middle panels) or absence (top panels) of ZM323881 after 24 hours. Tube formation was quantified by increased tube area by VEGF or HGF in the presence or absence of ZM323881 (bottom). $^{**}P < 0.01$.

required for Akt phosphorylation in HAECs, suggesting that VEGFR-2 is responsible for VEGF-Akt-induced cell migration.

ZM323881 completely inhibits VEGF-induced CrkII phosphorylation, indicating that CrkII phosphorylation depends on VEGFR-2. Although VEGFR-1 contains a potential CrkII SH2-binding motif (19), VEGFR-2 is responsible for VEGF-triggered CrkII signaling. Furthermore, phosphorylation of the CrkII SH2-binding protein $p130^{Cas}$ is also perturbed by ZM323881. VEGF-induced membrane extension was abrogated by either overexpression of dominant negative CrkII [Fig. 4(A)] or ZM323881 [Fig. 5(A)]. We have previously demonstrated that CrkII is involved in sphingosine 1-phosphate-induced cell motility via VEGFR-2 and that CrkII is required for ephrin-Eph-mediated membrane ruffling in vascular endothelial cells (21,32), suggesting that CrkII plays an pivotal role in endothelial cell migration. Taken together with these previous reports, our data here indicate that VEGF-induced membrane extension requires VEGFR-2-triggered CrkII signaling.

©2002 Marcel Dekker, Inc. All rights reserved. This material may not be used or reproduced in any form without the express written permission of Marcel Dekker, Inc.

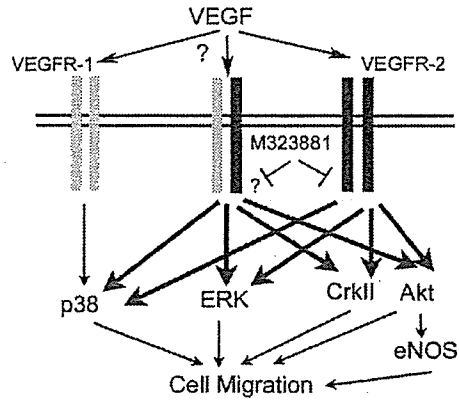

Figure 7. Vascular endothelial growth factor receptor-2-dependent signaling contributing to cell migration and the feasible role of a heterodimerized VEGFR-1 and VEGFR-2.

We have found that VEGF-induced ERK and p38 activation depends on VEGFR-2 in endothelial cells. ERK activation not only stimulates cell proliferation but promotes cell migration by phosphorylating myosin light chain kinase to enhance act-myosin-based contractility (33). Previous data demonstrated that p38 mediates actin reorganization and focal adhesion assembly in VEGF-stimulated endothelial cells (9). Thus, both ERK and p38 activated downstream of VEGFR-2 may contribute to cell migration of endothelial cells by modulating the actin cytoskeleton and cell attachment to extracellular matrices.

VEGFR-2 is required for VEGF-induced acceleration of cell migration [Fig. 5(B)] and in vitro tube formation on matrigel (Fig. 6). These results do not exclude the involvement of VEGFR-1 in angiogenesis in vivo. Carmeliet et al. (34) reported that PlGF is involved in enhancing VEGF-induced angiogenesis in ischemia, wound healing and tumor. This angiogenesis is attributed to the synergistic activation of VEGFR-2 by VEGF and VEGFR-1 by PlGF. PlGF may stimulate vascular smooth muscle cells in angiogenesis, since vascular smooth muscle cells do not express VEGFR-2 but upregulate matrix metalloproteinase expression contributing to cell migration in response to PlGF (35). Recently, in endothelial cells, matrices metalloproteinases have been shown to be required for tube formation in gels (36). Therefore, not only VEGFR-1 on vascular smooth muscle cells but those on endothelial cell may function as a contributor for anogiogenesis.

VEGFR-1 binds to VEGF with 10 times higher affinity than VEGFR-2. Therefore, homodimerized VEGFR-1 functions competitively with homodimerized VEGFR-2 for VEGF. In contrast to this notion, VEGFR-1 can heterodimerize with VEGFR-2 in response to VEGF to more efficiently promote cell migration and PI3-K activation than homodimerized VEGFR-2 in pulmonary aortic endothelial cells expressing both VEGFR-1 and VEGFR-2 (37,38). If VEGFR-2 could heterodimerize with VEGFR-1 in HAECs, ZM323881 might inhibit the signaling downstream to a heterodimer of VEGFR-2 and VEGFR-1 (Fig. 7). Very recently, PlGF is shown to activate VEGFR-2 via VEGFR-1 in a transactivation manner (39). Since PlGF-induced p38 phosphorylation was not inhibited by ZM323881 and PlGF was unable to induce ERK phosphorylation [Fig. 1(C) and (D)], a VEGFR-2/VEGFR-1 heterodimer may not function under these stimulation. Thus, to dissect the VEGFR-1/VEGFR-2 heterodimer-dependent signaling and VEGFR-2 homo-

©2002 Marcel Dekker, Inc. All rights reserved. This material may not be used or reproduced in any form without the express written permission of Marcel Dekker, Inc.

dimer-dependent signaling, a VEGFR-1 selective inhibitor would be a valuable tool to help to fully understand how VEGFR-1 and VEGFR-2 function and interact in angiogenesis.

In conclusion, ZM323881 is a novel VEGFR-2 inhibitor and delineates the angiogenic signaling downstream of VEGFR-2.

ACKNOWLEDGMENTS

This work was supported by the grant from the Ministry of Health, Labour, and Welfare Foundation of Japan, and by the grant of Bio-Venture Research Fund Project Aid from the Ministry of Education, Culture, Sports, Science and Technology of Japan, by the grant from the Promotion of Fundamental Studies in Health Science of the Organization for Pharmaceutical Safety and Research of Japan, by the grant from Suzuken Memorial Foundation, and by the grant from Mitsubishi Pharma Research Foundation.

REFERENCES

1. Yancopoulos GD, Davis S, Gale NW, Rudge JS, Wiegand SJ, Holash J. Vascular-specific growth factors and blood vessel formation. Nature 2000; 407(6801):242–248.
2. Shalaby F, Rossant J, Yamaguchi TP, Gertsenstein M, Wu XF, Breitman ML, Schuh AC. Failure of blood-island formation and vasculogenesis in Flk-1-deficient mice. Nature 1995; 376(6535):62–66.
3. Fong GH, Rossant J, Gertsenstein M, Breitman ML. Role of the Flt-1 receptor tyrosine kinase in regulating the assembly of vascular endothelium. Nature 1995; 376(6535):66–70.
4. Kaipainen A, Korhonen J, Mustonen T, van Hinsbergh VW, Fang GH, Dumont D, Breitman M, Alitalo K. Expression of the fms-like tyrosine kinase 4 gene becomes restricted to lymphatic endothelium during development. Proc Natl Acad Sci USA 1995; 92(8):3566–3570.
5. Bernatchez PN, Soker S, Sirois MG. Vascular endothelial growth factor effect on endothelial cell proliferation, migration, and platelet-activating factor synthesis is Flk-1-dependent. J Biol Chem 1999; 274(43):31047–31054.
6. Kroll J, Waltenberger J. The vascular endothelial growth factor receptor KDR activates multiple signal transduction pathways in porcine aortic endothelial cells. J Biol Chem 1997; 272(51):32521–32527.
7. Gille H, Kowalski J, Li B, LeCouter J, Moffat B, Zioncheck TF, Pelletier N, Ferrara N. Analysis of biological effects and signaling properties of Flt-1 (VEGFR- 1) and KDR (VEGFR-2). A reassessment using novel receptor-specific vascular endothelial growth factor mutants. J Biol Chem 2001; 276(5):3222–3230.
8. Chang L, Karin M. Mammalian MAP kinase signalling cascades. Nature 2001; 410(6824):37–40.
9. Rousseau S, Houle F, Landry J, Huot J. p38 MAP kinase activation by vascular endothelial growth factor mediates actin reorganization and cell migration in human endothelial cells. Oncogene 1997; 15(18):2169–2177.
10. Takahashi T, Yamaguchi S, Chida K, Shibuya M. A single autophosphorylation site on KDR/Flk-1 is essential for VEGF-A- dependent activation of PLC-gamma and DNA synthesis in vascular endothelial cells. EMBO J 2001; 20(11):2768–2778.

©2002 Marcel Dekker, Inc. All rights reserved. This material may not be used or reproduced in any form without the express written permission of Marcel Dekker, Inc.

11. Morales-Ruiz M, Fulton D, Sowa G, Languino LR, Fujio Y, Walsh K, Sessa WC. Vascular endothelial growth factor-stimulated actin reorganization and migration of endothelial cells is regulated via the serine/threonine kinase Akt. Circ Res 2000; 86(8):892–896.
12. Gerber HP, McMurtrey A, Kowalski J, Yan M, Keyt BA, Dixit V, Ferrara N. Vascular endothelial growth factor regulates endothelial cell survival through the phosphatidylinositol 3′-kinase/Akt signal transduction pathway. Requirement for Flk-1/KDR activation. J Biol Chem 1998; 273(46):30336–30343.
13. Shiojima I, Walsh K. Role of Akt signaling in vascular homeostasis and angiogenesis. Circ Res 2002; 90(12):1243–1250.
14. Lee MJ, Thangada S, Paik JH, Sapkota GP, Ancellin N, Chae SS, Wu M, Morales-Ruiz M, Sessa WC, Alessi DR, Hla T. Akt-mediated phosphorylation of the G protein-coupled receptor EDG-1 is required for endothelial cell chemotaxis. Mol Cell 2001; 8(3):693–704.
15. Bar-Sagi D, Hall A. Ras and Rho GTPases: a family reunion. Cell 2000; 103(2):227–238.
16. Kiyokawa E, Mochizuki N, Kurata T, Matsuda M. Role of Crk oncogene product in physiologic signaling. Crit Rev Oncog 1997; 8(4):329–342.
17. Kiyokawa E, Hashimoto Y, Kobayashi S, Sugimura H, Kurata T, Matsuda M. Activation of Rac1 by a Crk SH3-binding protein, DOCK180. Genes Dev 1998; 12(21):3331–3336.
18. Yano H, Uchida H, Iwasaki T, Mukai M, Akedo H, Nakamura K, Hashimoto S, Sabe H. Paxillin alpha and Crk-associated substrate exert opposing effects on cell migration and contact inhibition of growth through tyrosine phosphorylation. Proc Natl Acad Sci USA 2000; 97(16):9076–9081.
19. Ito N, Wernstedt C, Engstrom U, Claesson-Welsh L. Identification of vascular endothelial growth factor receptor-1 tyrosine phosphorylation sites and binding of SH2 domain-containing molecules. J Biol Chem 1998; 273(36):23410–23418.
20. Stoletov KV, Ratcliffe KE, Spring SC, Terman BI. NCK and PAK participate in the signaling pathway by which vascular endothelial growth factor stimulates the assembly of focal adhesions. J Biol Chem 2001; 276(25):22748–22755.
21. Endo A, Nagashima K, Kurose H, Mochizuki S, Matsuda M, Mochizuki N. Sphingosine 1-phosphate induces membrane ruffling and increases motility of human umbilical vein endothelial cells via vascular endothelial growth factor receptor and CrkII. J Biol Chem 2002; 277(26):23747–23754.
22. Kim YM, Kim YM, Lee YM, Kim HS, Kim JD, Choi Y, Kim KW, Lee SY, Kwon YG. TNF-related activation-induced cytokine (TRANCE) induces angiogenesis through the activation of Src and phospholipase C (PLC) in human endothelial cells. J Biol Chem 2002; 277(9):6799–6805.
23. Hennequin LF, Thomas AP, Johnstone C, Stokes ES, Plé PA, Lohmann JJ, Ogilvie DJ, Dukes M, Wedge SR, Curwen JO, Kendrew J, Lambert-van der Brempt C. Design and structure-activity relationship of a new class of potent VEGF receptor tyrosine kinase inhibitors. J Med Chem 1999; 42(26):5369–5389.
24. Whittles CE, Pocock TM, Wedge SR, Kendrew J, Hennequin LF, Harper SJ, Bates, DO ZM323881, a novel inhibitor of vascular endothelial growth factor-receptor-2 tyrosine kinase activity. Microcirculation 2002; 9(6):513–522.
25. Ferrara N, Davis-Smyth T. The biology of vascular endothelial growth factor. Endocr Rev 1997; 18(1):4–25.

©2002 Marcel Dekker, Inc. All rights reserved. This material may not be used or reproduced in any form without the express written permission of Marcel Dekker, Inc.

26. Shibuya M. Structure and function of VEGF/VEGF-receptor system involved in angiogenesis. Cell Struct Funct 2001; 26(1):25–35.
27. Lauffenburger DA, Horwitz AF. Cell migration: a physically integrated molecular process. Cell 1996; 84(3):359–369.
28. Bishop AL, Hall A. Rho GTPases and their effector proteins. Biochem J 2000; 348(Pt 2):241–255.
29. Toker A, Cantley LC. Signalling through the lipid products of phosphoinositide-3-OH kinase. Nature 1997; 387(6634):673–676.
30. Thakker GD, Hajjar DP, Muller WA, Rosengart TK. The role of phosphatidylinositol 3-kinase in vascular endothelial growth factor signaling. J Biol Chem 1999; 274(15):10002–10007.
31. Makinen T, Veikkola T, Mustjoki S, Karpanen T, Catimel B, Nice EC, Wise L, Mercer A, Kowalski H, Kerjaschki D, Stacker SA, Achen MG, Alitalo K. Isolated lymphatic endothelial cells transduce growth, survival and migratory signals via the VEGF-C/D receptor VEGFR-3. EMBO J 2001; 20(17):4762–4773.
32. Nagashima K, Endo A, Ogita H, Kawana A, Yamagishi A, Kitabatake A, Matsuda M, Mochizuki N. Adaptor protein Crk is required for ephrin-B1-induced membrane ruffling and focal complex assembly of human aortic endothelial cells. Mol Biol Cell 2002; 13(12):4231–4242.
33. Klemke RL, Cai S, Giannini AL, Gallagher PJ, de Lanerolle P, Cheresh DA. Regulation of cell motility by mitogen-activated protein kinase. J Cell Biol 1997; 137(2):481–492.
34. Carmeliet P, Moons L, Luttun A, Vincenti V, Compernolle V, De Mol M, Wu Y, Bono F, Devy L, Beck H, Scholz D, Acker T, DiPalma T, Dewerchin M, Noel A, Stalmans I, Barra A, Blacher S, Vandendriessche T, Ponten A, Eriksson U, Plate KH, Foidart JM, Schaper W, Charnock-Jones DS, Hicklin DJ, Herbert JM, Collen D, Persico MG. Synergism between vascular endothelial growth factor and placental growth factor contributes to angiogenesis and plasma extravasation in pathological conditions. Nat Med 2001; 7(5):575–583.
35. Wang H, Keiser JA. Vascular endothelial growth factor upregulates the expression of matrix metalloproteinases in vascular smooth muscle cells: role of flt-1. Circ Res 1998; 83(8):832–840.
36. Lafleur MA, Handsley MM, Knauper V, Murphy G, Edwards DR. Endothelial tubulogenesis within fibrin gels specifically requires the activity of membrane-type-matrix metalloproteinases (MT-MMPs). J Cell Sci 2002; 115(Pt17):3427–3438.
37. Huang K, Andersson C, Roomans GM, Ito N, Claesson-Welsh L. Signaling properties of VEGF receptor-1 and -2 homo- and heterodimers. Int J Biochem Cell Biol 2001; 33(4):315–324.
38. Kendall RL, Wang G, Thomas KA. Identification of a natural soluble form of the vascular endothelial growth factor receptor, FLT-1, and its heterodimerization with KDR. Biochem Biophys Res Commun 1996; 226(2):324–328.
39. Autiero M, Waltenberger J, Communi D, Kranz A, Moons L, Lambrechts D, Kroll J, Plaisance S, De Mol M, Bono F, Kliche S, Fellbrich G, Ballmer-Hofer K, Maglione D, Mayr-Beyrle U, Dewerchin M, Dombrowski S, Stanimirovic D, Van Hummelen P, Dehio C, Hicklin DJ, Persico G, Herbert JM, Communi D, Shibuya M, Collen D, Conway EM, Carmeliet P. Role of PlGF in the intra- and intermolecular cross talk between the VEGF receptors Flt1 and Flk1. Nat Med 2003; 9(7):936–943.

Control of COX-2 Gene Expression through Peroxisome Proliferator-Activated Receptor γ in Human Cervical Cancer Cells

Shouwei Han, Hiroyasu Inoue, Lisa C. Flowers, and Neil Sidell[1]

Division of Research, Department of Gynecology and Obstetrics, Emory University School of Medicine, Atlanta, Georgia 30322 [S. H., L. C. F., N. S.], and Department of Pharmacology, National Cardiovascular Center Research Institute, Osaka, 565-8565, Japan [H. I.]

ABSTRACT

Purpose: **The peroxisome proliferator-activated receptor-γ (PPARγ), a ligand-dependent transcription factor belonging to the family of nuclear receptors, has been implicated in the control of cyclooxygenase (COX) 2 expression in some tissue, although the exact mechanism(s) of this activity has not been elucidated. In this study we explored the possible mechanism(s) of control of COX-2 gene expression through PPARγ signaling in human cervical cancer.**

Experimental Design: **Using primary human cervical tissues and the CaSki human cervical cancer cell line, we assayed for PPARγ and COX-2 mRNA expression by reverse transcription-PCR. Nuclear protein binding activities to three response elements located in the COX-2 promoter [nuclear factor κB (NFκB), cyclic AMP response element, and activator protein (AP)-2] were measured by gel mobility shift assays. We used transient transfection assays with COX-2 promoter reporter gene constructs to determine the regulatory sites in this promoter, which mediates PPARγ regulation of COX-2 activity.**

Results: **We showed, for the first time, that primary human cervical cancer tissues express PPARγ. Using CaSki cells, we demonstrated that COX-2 and PPARγ mRNA levels were inversely regulated by PPARγ ligands in that these compounds up-regulated PPARγ but down-regulated COX-2. In contrast, epidermal growth factor (EGF), a potent activator of COX-2, decreased PPARγ mRNA levels. This down-regulation of PPARγ mRNA by EGF was blocked in the presence of NS-398, a selective COX-2 inhibitor. PPARγ ligands suppressed the binding activities of AP-1 (binding to CRE) and NFκB but not AP-2. Transient transfection results indicated that EGF stimulated whereas PPARγ ligands inhibited COX-2 promoter (−327/+59) activity. This effect by PPARγ ligands on the COX-2 promoter was blocked when the CRE, but not the NFκB, binding site was mutagenized.**

Conlcusion: **Cervical cancer cells express readily detectable levels of PPARγ. There is reciprocal negative regulation between COX-2 and PPARγ signaling in human cervical cancer cells. The ability of PPARγ ligands to inhibit COX-2 appears to be mediated predominantly through inhibition of AP-1 protein binding to the CRE site in the COX-2 promoter.**

INTRODUCTION

It has been generally accepted that there are two isoforms of COX.[2] COX-1 is expressed constitutively in most tissues and appears to be responsible for various physiological functions. COX-2, which is a key enzyme in prostaglandin synthesis, is an immediate, early response gene that is rapidly induced by phorbol esters, growth factors, cytokines, and oncogenes (1). COX-2 overexpression has been observed in many tumor types including colon, lung, breast, and esophagus (2, 3). Recent reports (4) have indicated that COX-2 is also overexpressed in human cervical cancer, the second leading cause of cancer deaths in women worldwide and a leading cause of mortality among women of reproductive age in developing countries (5). Mechanistic studies have suggested that expression of COX-2 in stage IB cervical cancer may down-regulate apoptotic processes and thus enhance tumor invasion and metastasis (6).

PPARs are ligand-dependent transcription factors belonging to the steroid hormone nuclear receptor superfamily (7, 8). The expression of PPARγ has been reported in several organs and tissues, such as liver, lung, skeletal muscle, and monocyte/macrophages, and at high levels in adipose tissue (9–11). Although PPARγ is expressed at low levels in normal colonic and breast ductal epithelium, it is increased significantly in both colon and breast carcinoma (12–14). The expression of this receptor in cervical tissue has heretofore not been reported.

PPARγ has been implicated in the regulation of critical aspects of development and homeostasis, including cell cycle control and tumor growth inhibition (8, 15). The PGD2 metabolite 15-deoxy-12, 14 PGJ2 (PGJ2) has been identified as a potent natural ligand for PPARγ and can be produced by overexpression of COX-2 (16). This fact suggests that PPARγ

Received 10/25/02; revised 4/28/03; accepted 5/9/03.
The costs of publication of this article were defrayed in part by the payment of page charges. This article must therefore be hereby marked *advertisement* in accordance with 18 U.S.C. Section 1734 solely to indicate this fact.

[1] To whom requests for reprints should be addressed, at Department of Gynecology and Obstetrics, Emory University School of Medicine, 1639 Pierce Drive, Atlanta, GA, 30322. Phone: (404) 727-9155; Fax: (404) 727-8615; E-mail: Nsidell@emory.edu.

[2] The abbreviations used are: COX, cyclooxygenase; PPAR, peroxisome proliferator-activated receptor; AP, activator protein; RT-PCR, reverse transcription-PCR; 15d-PGJ2, 15-deoxy-δ prostaglandin J_2; Cig, ciglitazone; NFκB, nuclear factor κB; GAPDH, glyceraldehyde-3-phosphate dehydrogenase; EMSA, electrophoretic mobility shift assay; EGF, epidermal growth factor; PUFA, polyunsaturated fatty acid.

signaling may be related to COX-2 gene expression. To this end, there are several reports suggesting a reciprocal interaction between COX-2 expression and PPARγ signaling. Thus, induction of COX-2 by 15d-PGJ2 was reported in immortalized epithelial and colorectal cancer cells (16, 17), although 15d-PGJ2 suppressed COX-2 expression in fetal hepatocytes (18). The molecular mechanism(s) that underlie PPARγ regulation of COX-2 expression remains to be elucidated. In this study, we investigated whether PPARγ signaling was involved in COX-2 regulation in human cervical cancer. Our data showed that PPARγ ligands can down-regulate COX-2 gene expression and that this regulation is mediated predominately through inhibition of the function of the AP-1 nuclear transcription factor.

MATERIALS AND METHODS

Patient Samples. Cervical cancer samples were collected for RT-PCR analysis from patients with different histological types: squamous cell carcinoma (n = 7) and adenocarcinoma (n = 1). Histologically normal cervical tissue samples were obtained from patients undergoing gynecological surgery at Grady Hospital/Emory University School of Medicine (Atlanta, GA). Samples were stored at −80°C until analysis. Informed consent was obtained from each patient. This study was approved by the Committees on Human Rights in Research at Emory University.

Cell Culture and Chemicals. The CaSki human cervical cancer cell line obtained from American Type Culture Collection (Manassas, VA) was grown in RPMI 1640 (Cellgro, Herndon, VA) supplemented with 10% heat-inactivated fetal bovine serum, HEPES buffer, 50 IU/ml penicillin/streptomycin, and 1 μg amphotericin (complete medium) as described previously (19). Murine 3T3-L1 cells obtained from American Type Culture Collection were grown in complete medium and were induced to differentiate into adipocytes by standard procedures (20). These "adipocyte-differentiated" 3T3-L1 cells were used for comparing PPARγ expression in adipocytes *versus* cervical cancer cells. 15d-PGJ2 and Cig were purchased from Alexis Biochemical (San Diego, CA) dissolved in methyl acetate and ethanol, respectively. GW1929 and GW9662 (21, 22) were synthesized by the Medicinal Chemistry Department at Glaxo Wellcome Research and Development and were generous gifts from Dr. Timothy M. Willson at same Institute (Glaxo Wellcome Co., Research Triangle Park, NC). The selective COX-2 inhibitor NS-398 (23) was obtained from Cayman Chemical (Ann Arbor, MI). Recombinant human EGF purchased from R&D systems (Minneapolis, MN) was dissolved in 10 μM acetic acid. Poly(deoxyinosinic-deoxycytidylic acid) was purchased from Amersham Pharmacia Biotech (Piscataway, NJ). NFκB, AP-1, CRE, and AP-2 oligouncleotides were purchased from Santa Cruz Biotechnology (San Diego, CA); 5′ DNA Terminus Labeling System was purchased from Life Technologies, Inc. (Rockville, MD). [γ-^{32}P]dATP was purchased from Perkin-Elmer Life Sciences, Inc. (Boston, MA). All of the RT-PCR kit components were from Perkin-Elmer Co. (Foster City, CA). All of the other chemicals were purchased from Sigma (St. Louis, MO) unless otherwise indicated.

RT-PCR. Total RNA was prepared from primary human cervical tissues and cultured CaSki cells by using TRIzol Reagent (Life Technologies, Inc.) according to the manufacturer's instructions. To amplify 474-bp PPARγ, 282-bp COX-2, and 200-bp GAPDH cDNA fragments, the sequences of PCR primers synthesized by Genosys (The Woodlands, Texas) were: for PPARγ sense (5′-TCTCTCCGTAATGGAAGACC-3′), antisense (5′-GCATTATGAGACATCCCCAC-3′); for COX-2 sense (5′-CTGTATCCCGCCCTGCTGGTG-3′), antisense (5′-ACTTGCGTTGATGGTGGCTGTCTT-3′); and for GAPDH sense (5′-CCATGGAGAAGGCTGGGG-3′), antisense (5′-CAAAGTTGTCATGGATGACC-3′) as according to the published data (24, 25). The RT-PCR was carried out as described (24). The samples were first denatured at 95°C for 30 s, followed by 32 PCR cycles, each with temperature variations as follows: 95°C for 30 s, 60°C for 30 s, and 72°C for 30 s. The last cycle was followed by an additional extension incubation of 7 min at 72°C. Analysis of amplicons was accomplished on 1% agarose gel containing 0.2 μg/μl ethidium bromide and visualized under UV transiluminator. The densitometric analysis of PCR products was performed by the computer software (Bio-Rad Quantity One), GS-700 Imaging Densitometer (Bio-Rad, Hercules, CA), and standardized by the GAPDH product. Ratio of PPARγ:GAPDH or COX-2:GAPDH density bands in control group was considered as 100%. Values of treatment group PPARγ:GAPDH or COX-2:GAPDH ratios are given as a percentage of controls. A 100-bp ladder (Life Technologies, Inc.) was used as a size standard.

For real-time PCR, the treatment and total RNA preparations were the same as those for the RT-PCR procedures described above. All of the PCR reactions using LightCycler-FastStart DNA Master SYBR Green I kit were performed in the Cepheid Smart-Cycler real-time PCR cycler (Sunnyvale, CA). The cycling conditions were as follows: initial denaturation at 95°C for 10 min, followed by 40 cycles at 95°C for 15 s, 60°C for 5 s, and 72°C for 10 s. Primers for PPARγ and GAPDH were the same as shown above. Primers used for detection of PPARγ in mouse 3T3-L1 cells were sense (5′-CGACTGCTGGTTGACACAGAGATGC-3′) and antisense (5′-CGAGATCTGGCCATGAGGGAGTTAG-3′). Quantitative analysis for determining threshold cycle for each sample was performed according to the vendor guidelines. Experiments were performed in triplicate for each data point. For all of the experiments, controls without templates were included.

EMSA. Nuclear protein extracts from CaSki cells were prepared for EMSA as described earlier (26). The protein content of the nuclear extract was determined using the bicinchoninic acid protein assay kit (Sigma). EMSA experiments were performed using double-stranded oligonucleotides comprising the consensus sequences (italicized) for NFκB (5′-AGTTGA*GGGGACTTTCCC*AGGC-3′), CRE (5′-AGAGATTGCC*TGACGTCA*GAGAGCTAG-3′), AP-1 (5′-GCTTGA*TGACTCA*GCCGGAA-3′), and AP-2 (5′-GATCGAACTGAC*CGCCCGCG*CCCCGT-3′). The binding site for CRE comprised the cyclic AMP-responsive element. The NFκB, CRE, and AP-2 oligonucleotides were end labeled with [γ-^{32}P]dATP using T4 polynucleotide kinase as recommended by the manufacturer. In the mutated NFκB oligonuclcotide, the consensus motif was changed to GGcGACTTTCCC. For mutated CRE and AP-2 oligonucleotides, the consensus motifs were changed to TGACTtg and CGCttGCGC, respectively. Five μg nuclear pro-

teins from control and treated cells were incubated with ^{32}P-labeled oligonucleotide probe under binding conditions [10 mM HEPES, Tris-HCL (pH 7.9), 50 mM KCl, 0.1 mM EDTA, 1 mM DTT, 12% (v/v) glycerol, and 2 μg poly(deoxyinosinic-deoxycytidylic acid)] for 20 min at room temperature in a final volume of 20 μl. For cold competition, a 100-fold excess of the respective unlabeled consensus oligonucleotides was added with the probe. The same amount of mutated oligonucleotides added with the probe was used as another control. All of these were in the same binding conditions as described before. After binding, protein-DNA complexes were electrophoresed on a native 4.5% polyacrylamide gel at 120 V using 1× Tris-Glycine buffer [10× Tris-glycine: Tris-base 30.28 g, glycine 142.7 g, EDTA 3.92 g, and H_2O added up to 1 liter (pH 8.5)]. Each gel was then dried and subjected to autoradiography at −80°C for up to 72 h. All of the vehicle controls were considered as 100%. Value of treatment groups was given as percentage of controls.

Plasmids. The COX-2 promoter constructs ligated to luciferase (−327/+59, KBM, CRM, and KBM+CRM) has been reported previously (27). Among those, KBM represents the −327/+59 COX-2 promoter construct in which the NFκB site (−223/−214) was mutagenized; CRM refers to the −327/+59 COX-2 promoter construct in which the CRE site (−59/−53) was mutagenized; KBM+CRM represent the −327/+59 COX-2 promoter construct in which the both NFκB and CRE sites were mutagenized. Synthetic Renilla Luciferase Report Vector (phRL-TK) was obtained from Promega.

Transient Transfection Assays. CaSki cells were seeded at a density of 4 × 10^4 cells/well in six-well dishes and grown to 50–60% confluence. For each well, 2 μg of plasmid DNA of the above constructs and 0.3 μg of the internal control plasmid pRL-TK (renilla luciferase gene) were cotransfected into the cells using 3 μl of FUGENE 6 lipofection reagent (Roche Molecular Biochemicals, Indianapolis, IN) as performed in our earlier work (28). After 24 h of incubation, cells were treated with PPARγ ligands (GW1929 and Cig), EGF, or solvent control for another 24 h. The preparation of cell extracts and measurement of luciferase activities were carried out using the Dual-Luciferase Reporter kit according to recommendations of the manufacturer (Promega). The assays for firefly luciferase activity and renilla luciferase activity were performed sequentially using one reaction tube in a luminometer with one injector. Changes in firefly luciferase activity were calculated and plotted after normalization with changes in renilla luciferase activity in the same sample. All of the vehicle controls were considered as 100%. Values of treatment group firefly luciferase:renilla luciferase ratio were given as percentage of controls.

Statistical Analysis. All of the experiments were repeated a minimum of three times. All of the gel shift assays, luciferase activity assays, and RT-PCR data were expressed as a mean ± SE. The data in some figures are from a representative experiment, which was qualitatively similar in the replicate experiments. Statistical significance was determined with Student's *t* test (two-tailed) comparison between two groups of data set. Asterisks shown in the figures indicate significant differences of experimental groups in comparison with the corresponding control condition ($P \leq 0.05$; see figure legends).

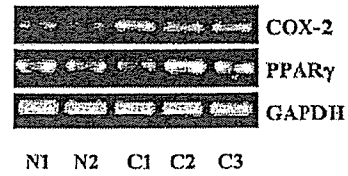

Fig. 1 Expression of COX-2 and PPARγ in normal and malignant cervical tissues obtains from patients undergoing gynecological surgery. Total RNA was isolated, and then subjected to RT-PCR analysis using PPARγ and COX-2 primers. *N* indicates normal tissue; *C* indicates cancer tissues. The numbers were given sequentially to normal and cancer patient samples, and do NOT indicate matched pairs from the same patient. Primers for GAPDH were used as an internal control for normalization purposes.

RESULTS

Expression of COX-2 and PPARγ Genes in Human Primary Cervical Cancer Cells and Cell Lines. Although recent reports have demonstrated overexpression of COX-2 activity in human cervical cancer cells, there are presently no reported studies showing the presence of PPARγ in this malignancy. As exemplified in Figs. 1 and 2, RT-PCR analysis indicated that PPARγ was readily detected in both human primary cervical cancer as well as the CaSki cervical cancer cell line. In addition, Fig. 1 shows relatively high expression of both COX-2 and PPARγ in malignancies, whereas COX-2 expression was low in nonmalignant samples. Similar results were obtained in a total of 8 cervical cancer and 13 normal tissue samples. To compare PPARγ mRNA levels in cervical cancer to that in adipose tissue, which are known to express very high levels of PPARγ (29), real-time RT-PCR was performed on CaSki cells and adipocyte-differentiated mouse 3T3-L1 cells (30). Results showed that the steady-state levels of PPARγ mRNA in adipocyte-differentiated 3T3-L1 was ~1000-fold greater than that found in CaSki. These findings represent the first report that PPARγ is expressed in either normal or malignant cells of the cervix.

Regulation of COX-2 Expression and its Link to PPARγ Signaling. In previous dose-response studies by one of us (H. I.) as well as by others (31, 32), it was shown that significant modulation of COX-2 levels in a variety of cell systems can be consistently induced by PPARγ ligands at concentrations of 10–50 μM. Preliminary experiments demonstrated that modulation of COX-2 by PPARγ ligands in CaSki cervical cancer cells showed a similar dose dependency (data not shown). Therefore, 20 μM of PPARγ ligands were used in many of the following experiments. Fig. 2*A* shows that treatment of CaSki cells with 15d-PGJ2 and GW1929 (20 μM each) for 5 h significantly induced PPARγ mRNA levels, whereas EGF (20 ng/ml) remarkably inhibited the expression of PPARγ as compared with the controls. In contrast, the PPARγ ligands decreased COX-2 mRNA levels, whereas EGF, a known activator of COX-2 (4), enhanced COX-2 expression (Fig. 2). Next we determined whether COX-2 signaling was directly involved in the inhibition of PPARγ expression caused by EGF treatment. As shown in Fig. 2*B*, this was indeed the case; down-regulation of PPARγ mRNA levels induced by EGF was blocked in the presence of NS-398, a selective COX-2 inhibitor, at a concen-

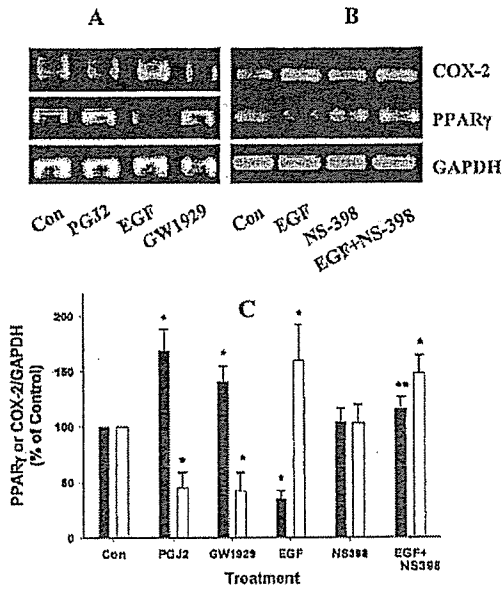

Fig. 2 Coordinated regulation of COX-2 and PPARγ expression in cervical cancer cells. Total RNA was isolated from CsSki cells cultured for 5 h with solvent control (*Con*) or the indicated compounds: (*A*) 20 μM 15d-PGJ2 or GW1929 or 20 ng/ml EGF; (*B*) 20 ng/ml EGF or 10 μM NS-398 or 10 μM NS-398 for 1 h followed by 20 ng/ml EGF for 5 h, then subjected to RT-PCR analysis using PPARγ, COX-2, and GAPDH primers. The bar graph (*C*) represents the mean PPARγ/GAPDH (■) or COX-2/GAPDH (□) band densities of at least three independent experiments; *bars*, ±SD. * indicates significant differences as compared with the vehicle control. ** indicates a significant difference after combination treatment as compared with treatment with EGF alone. NS-398 is known to block COX-2 activity, not COX-2 expression as reflected by no decrease in COX-2 mRNA levels in cells treated with this inhibitor.

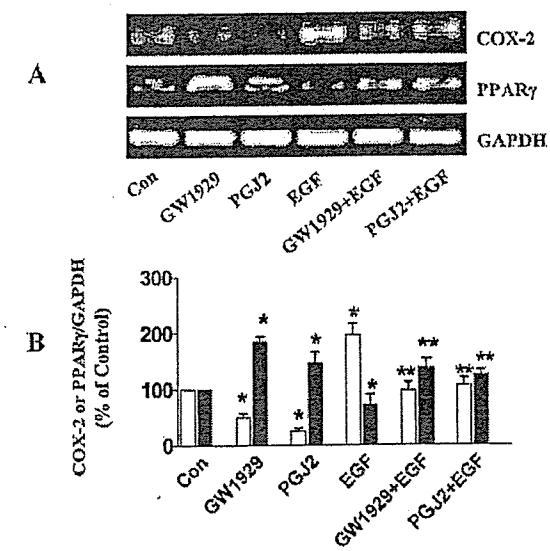

Fig. 3 Interaction between PPARγ and EGF signaling. Total RNA was isolated from CsSki cells cultured for 5 h with vehicle control (*Con*), 20 μM GW1929 or 15d-PGJ2, 20 ng/ml EGF, or 20 μM GW1929 or 15d-PGJ2 + 20 ng/ml EGF as indicated, then analyzed for PPARγ and COX-2 mRNA levels by RT-PCR. GAPDH mRNA expression was used as an internal control for normalization purposes (*A*). The bar graph (*B*) represents the mean PPARγ/GAPDH (■) or COX-2/GAPDH (□) band densities of at least three independent experiments; *bars*, ±SD. * indicates significant differences as compared with the vehicle control. ** indicates a significant difference after combination treatment as compared with treatment with EGF alone.

tration of 100 μM. In other experiments, PPARγ ligands GW1929 and 15d-PGJ2 at a concentration of 20 μM blocked EGF induction of COX-2 mRNA and suppression of PPARγ mRNA (Fig. 3), additionally suggesting that suppression of COX-2 could be mediated by PPARγ activation. Taken together, these findings suggest a reciprocal interaction between PPARγ and COX-2 regulation in cervical cancer cells.

AP-1 and NFκB Binding Activities Were Inhibited by PPARγ Ligands. To additionally elucidate the mechanisms responsible for the changes in amounts of COX-2 mRNA, EMSA was performed to identify the nuclear transcription factors that mediated the regulation of COX-2 mRNA by PPARγ ligands and EGF. The human COX-2 promoter region contains multiple transcription factor binding sites including a cyclic AMP response element (CRE), and binding motifs for NFκB and nuclear factor interleukin-6 (27, 33). Reports showed that AP-1 protein could bind to the CRE site located in the COX-2 promoter region (31). In agreement with other studies (34–36), CaSki cells treated with EGF (20 ng/ml) for 24 h slightly increased AP-1 and NFκB binding activity as compared with solvent controls. There was no binding activity when the CRE or NFκB sites were mutagenized (Figs. 4 and 5). In contrast, 15d-PGJ2 and GW1929 (20 μM each) inhibited AP-1 and NFκB binding as compared with controls. Inhibitory effects on AP-1 by these ligands were blocked in the presence of the PPARγ antagonist GW9662 (20 μM), whereas GW9662 alone had no effect on AP-1 binding activity (Fig. 6). These findings additionally indicated that the inhibitory effects of 15d-PGJ2 and GW1929 were mediated through the PPARγ signaling pathway. Additional experiments were performed to investigate the specificity of these PPARγ ligands on AP-1 and NFκB binding by assessing their effects on AP-2 binding activity. An AP-2 binding motif is also known to be located in the COX-2 promoter (37). Fig. 7 shows that 15d-PGJ2 and GW1929 had little effect on AP-2 binding. As a result of competition assays, specific bands for AP-1 (Fig. 6), NFκB (Fig. 5), and AP-2 (Fig. 7) were attenuated by a 100-fold molar excess of unlabeled oligonucleotides. These results confirmed that the nuclear protein binding to CRE is AP-1 and that the PPARγ ligands (15d-PGJ2 and GW1929) specifically inhibited the binding levels of both AP-1 and NFκB transcription factor complexes in human cervical cancer cells.

The CRE Binding Site in the COX-2 Promoter Plays a Major Role in the Effects of PPARγ Ligands. To define the regions of the COX-2 promoter that responded to EGF and PPARγ ligands, transient transfections were performed with human COX-2 promoter constructs. As shown in Fig. 8, EGF (20 ng/ml) treatment caused 4–5-fold increase in COX-2 promoter (−327/+59) activity, whereas the activity was suppressed

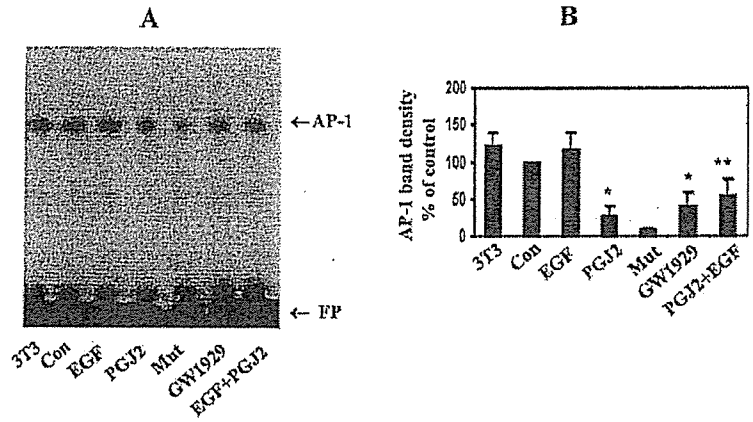

Fig. 4 Regulation of AP-1 binding activity in cervical cancer cells. Nuclear extracts were prepared from CaSki cells treated for 24 h with the compounds as indicated: solvent control (*Con*), 20 ng/ml EGF, 20 μM 15d-PGJ2 or GW1929, or 20 μM 15d-PGJ2 + 20 ng/ml EGF. Nuclear extracts were subjected to EMSA using a CRE consensus site radiolabeled probe and protein-DNA complexes were visualized by autoradiography (*A*). NIH 3T3 cells were used as a positive control (*3T3*); the CRE probe was mutagenized to show specificity of binding (*Mut*); *FP* indicates free probe. The bar graph (*B*) represents the mean of relative AP-1 binding as quantified by densitometry of at least three independent experiments for each treatment condition; *bars*, ±SD. * indicates significant difference as compared with the vehicle control. ** indicates significance of combination treatment as compared with single treatment values.

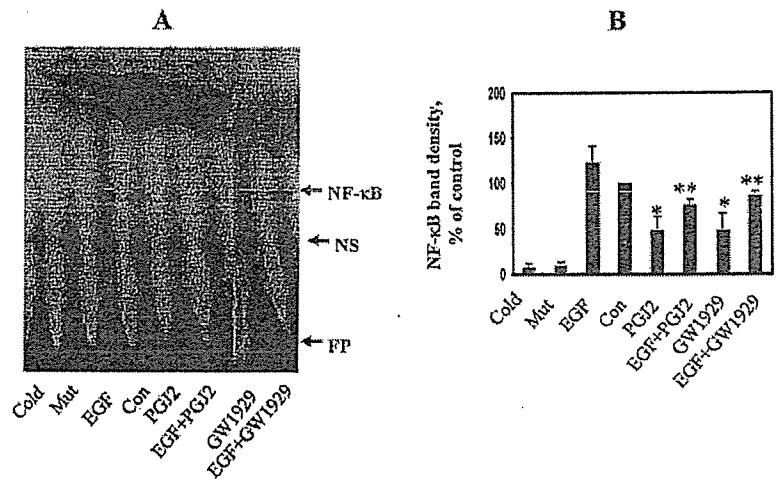

Fig. 5 Regulation of NFκB binding activity in cervical cancer cells. Nuclear extracts were prepared from CaSki cells treated for 24 h with the indicated compounds as described in Fig. 4 with the additional condition of 20 μM GW1929 + 20 ng/ml EGF. The extracts were then subjected to EMSA using a NFκB consensus site radiolabeled probe and protein-DNA complexes were visualized by autoradiography (*A*). A 100-fold molar excess of unlabeled (*Cold*) NFκB oligonucleotide was incubated with the radiolabeled probe/extract mixture for competition. The NFκB probe was mutagenized to show specificity of binding (*Mut*). *FP* indicates free probe; *NS* indicates a nonspecific band. The bar graph (*B*) represents the mean of relative NFκB binding as quantified by densitometry of at least three independent experiments for each treatment condition; *bars*, ±SD. * indicates significant difference as compared with the vehicle control. ** indicates significance of combination treatments as compared with the corresponding single treatment values.

to 35–40% of control in the presence of GW1929 or Cig. To additionally test for specific elements that are responsible for mediating the effect of EGF and PPARγ ligands, transient transfections were performed using COX-2 promoter constructs in which the CRE, NFκB, or both binding sites were mutagenized. As shown in Fig. 9, mutagenizing the NFκB site (KBM construct) caused some decrease in responsiveness to EGF, but no significant effect on GW1929 or Cig inhibitory responses. However, mutagenizing the CRE site (CRM) caused a marked inhibition of responses to GW1929 and Cig, as well as to induction by EGF. Mutations of both the CRE and NFκB binding sites almost completely blocked the EGF-dependent promoter activation and totally blocked the PPARγ ligand-suppressive effect on COX-2 promoter activity.